

The effect of interface phonons on operating electron states in three-barrier resonant tunneling structure as an active region of quantum cascade detector

M.V. Tkach*, Ju.O. Seti, Y.B. Grynyshyn, O.M. Voitsekhivska

Chernivtsi National University, 2 Kotsubynsky St., 58012 Chernivtsi, Ukraine

Received April 16, 2014, in final form May 17, 2014

The Hamiltonian of electrons interacting with interface phonons in three-barrier resonant tunneling structure is established using the first principles within the models of effective mass and polarization continuum. Using the Green's functions method, the temperature shifts and decay rates of operating electron states are calculated depending on geometric design of three-barrier nano-structure GaAs/Al_xGa_{1-x}As which is an active region of quantum cascade detector. It is established that independently of the temperature, the energy of quantum transition during the process of electromagnetic field absorption is a nonlinear weakly varying function of the position of the inner barrier with respect to the outer barriers of the structure.

Key words: resonant tunneling nano-structure, interface phonons, quantum cascade detector

PACS: 78.67.De, 63.20.Kr, 72.10.Di

1. Introduction

Quantum cascade detectors (QCD) have been investigated for over a decade but a growing attention to these devices is still observed [1–4]. From practical point of view, such an interest is caused by the unique characteristics of QCD. Occupying the whole infrared and terahertz frequency range of electromagnetic waves, these devices can operate in a wide range of temperatures (from cryogenic to room ones) and so on. From theoretical point of view, the interest is caused by the fact that the basis of QCD functional elements are the open quasi-two-dimensional resonant tunneling structures (RTS). The physical properties of electronic transport in these structures are not still clear enough.

The theory of spectral parameters and dynamic conductivity of electrons in open RTS is well developed [5–7] without taking into account the electron-phonon interaction. The obtained results well correlate with the experimental data [3]. However, from physical considerations it is clear that the effect of phonons can be neglected only at cryogenic temperatures when the average occupation numbers of phonon states are small and electron-phonon binding is weak. Studying the nano-structures with strong binding or at high temperatures (modern QCDs operate at room temperatures [3]), one should consider the electron-phonon interaction.

The theory of electron-phonon interaction in spherical, cylindrical and plane closed single [8, 9] and multi-shell nano-heterosystems [10–15] has been developed for a long time using the models of effective mass and dielectric continuum. It was established that, contrary to the massive three-dimensional systems, the so-called interface phonons (I-phonons) exist in low-dimensional nano-heterosystems (besides the confined polarization phonons). The effect of I-phonons increases when the thickness of nano-layers decreases.

The effect of phonons on the transport properties of electronic current through RTS was mainly investigated for the two- and three-barrier nano-structures [5–7]. Studying the probabilities of quantum

*E-mail: ktf@chnu.edu.ua

transitions using the Fermi golden rule, it is enough to use the Hamiltonian of electron-phonon interaction in the representation of the second quantization over the phonon variables only, obtained by Mori and Ando [8] for a double heterostructure.

In this study, we investigate the electron spectrum renormalized due to I-phonons in three-barrier RTS which is an active region of QCD. The Hamiltonian of electron-I-phonon system is obtained in the representation of occupation numbers over all variables. It is further used in the method of temperature Green's functions in order to study the shifts and decay rates of two lower electron states - the operating states of QCD active region. This makes it possible to study in detail the effect of various mechanisms of electron-I-phonon interaction on the parameters of two operating electron states depending on the design of three-barrier RTS at cryogenic and room temperatures.

2. Hamiltonian and Fourier image of Green's function of the system of electrons interacting with interface polarization phonons in a three-barrier nano-structure

The theory of spectral parameters (resonance energies and decay rates) and dynamic conductivity of electrons in three-barrier RTS without taking into account the electron-phonon interaction was developed in detail in [5]. It was established that when the widths of nano-structure outer barriers were bigger than 3–4 nm, the resonance energies in open and closed models were almost the same and the resonance widths were two-three orders smaller than the energies. Considering the widths of outer barriers of a three-barrier RTS (the active bands of experimental QCD) as rather big (3–6 nm) [6], we develop the theory of electron-I-phonon interaction using the model of closed three-barrier RTS (figure 1) with fixed effective masses $m(z) = \{m_w(\text{II, IV}); m_b(\text{I, III, V})\}$ and rectangular potential energy profile neglecting the small decay rate

$$U(z) = \begin{cases} 0, & 0 \leq z \leq a_1 \text{ (II)}, & a_1 + b \leq z \leq a_1 + b + a_2 \text{ (IV)}, \\ U, & -\infty \leq z \leq 0 \text{ (I)}, & a_1 \leq z \leq a_1 + b \text{ (III)}, & a_1 + b + a_2 \leq z \leq \infty \text{ (V)}. \end{cases} \quad (1)$$

Expressing the electron wave function in the form

$$\Psi_{E\vec{k}}(\vec{r}) = \frac{1}{\sqrt{S}} e^{i\vec{k}\vec{\rho}} \Psi_E(z), \quad (2)$$

where \vec{k} and $\vec{\rho}$ are quasi-momentum and radius-vector of electron in the plane xOy and S is the square of the main region in this plane. For z -th component of this function, we obtain the Schrodinger equation

$$\left\{ -\frac{\hbar^2}{2} \frac{d}{dz} \frac{1}{m(z)} \frac{d}{dz} + U(z) \right\} \Psi_E(z) = E \Psi_E(z). \quad (3)$$

The complete electron energy in the region under the barrier ($E \leq U$) consists of two terms

$$E_{n\vec{k}} = E_n + \frac{\hbar^2 k^2}{2m_n^*}. \quad (4)$$

Here, $\hbar^2 k^2 / (2m_n^*)$ is the kinetic energy of electron moving in the plane perpendicular to Oz axis. It is determined, as in [16], by the effective mass correlated over the RTS

$$\frac{1}{m_n^*} = \int_{-\infty}^{\infty} \frac{|\Psi_n(z)|^2 dz}{m(z)}, \quad (5)$$

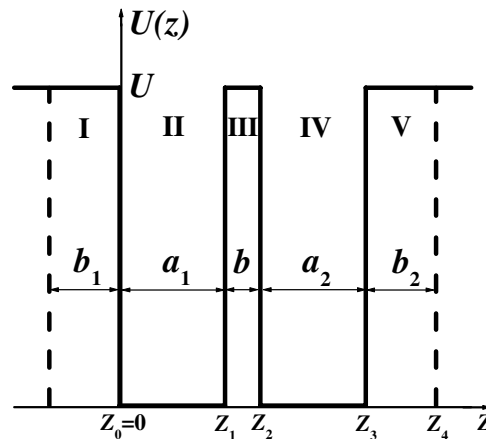


Figure 1. Potential energy profile of closed three-barrier RTS (solid line). The boundaries of outer barriers with the widths (b_1 ; b_2) for the corresponding open system (dashed lines).

where $\Psi_n(z)$ wave functions are the solutions of one-dimensional stationary equation (3)

$$\Psi_n(z) = \begin{cases} \sum_{j=2,4} \Psi_{jn}(z) = \sum_{j=2,4} (A_{jn} \cos k_n z + B_{jn} \sin k_n z), \\ \sum_{j=1,3,5} \Psi_{jn}(z) = \sum_{j=1,3,5} (A_{jn} e^{\chi_n z} + B_{jn} e^{-\chi_n z}). \end{cases} \quad (6)$$

Here,

$$k_n = \hbar^{-1} \sqrt{2m_w E_n}, \quad \chi_n = \hbar^{-1} \sqrt{2m_b |U - E_n|} = \sqrt{2m_b U \hbar^{-2} - k_n^2 m_b / m_w}. \quad (7)$$

The discrete energy spectrum E_n and coefficients A_{jn} , B_{jn} are fixed by fitting conditions

$$\begin{cases} \Psi_{jn}(z)|_{z=z_j} = \Psi_{j+1,n}(z)|_{z=z_j}, \\ \frac{1}{m_j} \frac{\partial \Psi_{jn}}{\partial z} \Big|_{z=z_j} = \frac{1}{m_{j+1}} \frac{\partial \Psi_{j+1,n}}{\partial z} \Big|_{z=z_j}, \quad j = 1, 2, 3, 4 \end{cases} \quad (8)$$

together with the condition that the wave function vanishes at $z \rightarrow \pm\infty$ ($B_{1n} = A_{5n} = 0$) and the normality condition

$$\int_{-\infty}^{\infty} \Psi_n^*(z) \Psi_{n'}(z) dz = \delta_{nn'}. \quad (9)$$

In the region above the barrier ($E \geq U$), the energy of electron longitudinal movement is continuous. Thus, introducing the longitudinal quasi-momentum k_z , it is written as $E_{k_z} = \hbar^2 k_z^2 / (2m_w)$. Finally, the complete energy has the form:

$$E_{k_z \bar{k}} = E_{k_z} + \frac{\hbar^2 k^2}{2m_w}. \quad (10)$$

Now, the solution of equation (3) for the wave function $\Psi_{k_z}(z)$ becomes the expression (6) with $k_n \rightarrow k_z$, $\chi_n \rightarrow i\chi$. The fitting conditions (8) are valid at $n \rightarrow k_z$, and the normality condition, similarly to the de Broglie wave, is written as follows:

$$\int_{-L/2}^{L/2} |\Psi_{k_z}(z)|^2 dz = 1, \quad (11)$$

where $\Psi_{k_z}(z)$ function satisfies the periodic condition $\Psi_{k_z}(-L/2) = \Psi_{k_z}(L/2)$ at a big span of the main region having the length L . All coefficients (A_{jk_z} , B_{jk_z}) are defined from these conditions and the wave function $\Psi_{k_z}(z)$ is obtained.

Introducing the generalized index $\bar{n} = \begin{cases} n, & E \leq U \\ k_z, & E \geq U \end{cases}$, for the compact analytics, we perform a transition to the representation of the second quantization using the quantized wave function

$$\widehat{\Psi}(\vec{r}) = \sum_{\bar{n}\bar{k}} \Psi_{\bar{n}\bar{k}}(\vec{\rho}, z) \widehat{a}_{\bar{n}\bar{k}} = \sum_{\bar{k}} \left[\sum_n \Psi_n(\vec{\rho}, z) a_{n\bar{k}} + \sum_{k_z} \Psi_{k_z}(\vec{\rho}, z) a_{k_z \bar{k}} \right] \quad (12)$$

and obtain the Hamiltonian of uncoupling electrons in the representation of their occupation numbers

$$\widehat{H}_e = \sum_{\bar{n}, \bar{k}} E_{\bar{n}\bar{k}} a_{\bar{n}\bar{k}}^+ a_{\bar{n}\bar{k}} \quad (13)$$

with the electron spectrum $E_{\bar{n}\bar{k}}$, creation ($a_{\bar{n}\bar{k}}^+$) and annihilation ($a_{\bar{n}\bar{k}}$) Fermi operators of electron states, satisfying the anti-commutative relationships.

It is well known [8–10] that in the dielectric continuum model, the phonon spectra and potential of polarization field $\Phi(\vec{r})$ are obtained from the following equation

$$\varepsilon_j(\omega) \nabla^2 \Phi(\vec{r}) = 0, \quad (14)$$

where $\varepsilon_j(\omega)$ is dielectric constant of j -th layer of a nano-structure composed of two materials

$$\varepsilon_j(\omega) = \varepsilon_{j\infty} \frac{\omega^2 - \omega_{Lj}^2}{\omega^2 - \omega_{Tj}^2}. \quad (15)$$

Here, $\varepsilon_{j\infty}$ is high-frequency dielectric constant, ω_{Lj} , ω_{Tj} are the frequencies of longitudinal (L) and transversal (T) phonons of the bulk material creating j -th layer of nano-structure.

The spectrum and potential of polarization field of interface phonons is obtained, according to [9], from the equation (14) if

$$\nabla^2 \Phi(\vec{r}) = 0. \quad (16)$$

Thus, the solution of this equation is the potential

$$\Phi(\vec{r}) = \sum_{j, \vec{q}} C(q) \varphi_j(q, z) e^{i\vec{q}\vec{\rho}}, \quad (17)$$

where \vec{q} , $\vec{\rho}$ are two-dimensional vectors and functions

$$\varphi_j(q, z) = \alpha_j e^{-qz} + \beta_j e^{qz}, \quad j = 1, \dots, 5 \quad (18)$$

satisfy the system of equations obtained from the fitting conditions for the intensity and induction of polarization field

$$\begin{cases} \varphi_j(q, z_j) = \varphi_{j+1}(q, z_j), \\ \varepsilon_j(\omega) \frac{\partial \varphi_j(q, z)}{\partial z} \Big|_{z=z_j} = \varepsilon_{j+1}(\omega) \frac{\partial \varphi_{j+1}(q, z)}{\partial z} \Big|_{z=z_j}, \end{cases} \quad j = 1, 2, 3, 4 \quad (19)$$

and considering that at $z \rightarrow \pm\infty$

$$\varphi_1(q, z) \Big|_{z \rightarrow -\infty} = \varphi_5(q, z) \Big|_{z \rightarrow \infty} = 0. \quad (20)$$

Within the transfer-matrix method [11], the coefficients α_j , β_j and the potential of polarization field $\Phi(\vec{r})$ are obtained from the system of equations (19), (20). The condition of nontrivial solution determines the dispersion equation

$$\prod_{j=1}^5 \begin{pmatrix} \left[1 + \frac{\varepsilon_1(\Omega)}{\varepsilon_0(\Omega)} \right] & \left[1 - \frac{\varepsilon_1(\Omega)}{\varepsilon_0(\Omega)} \right] e^{-2qz_{j-1}} \\ \left[1 - \frac{\varepsilon_1(\Omega)}{\varepsilon_0(\Omega)} \right] e^{2qz_{j-1}} & \left[1 + \frac{\varepsilon_1(\Omega)}{\varepsilon_0(\Omega)} \right] \end{pmatrix} = \begin{pmatrix} 1 & 0 \\ 0 & 1 \end{pmatrix}. \quad (21)$$

Here, $\varepsilon_0(\Omega)$ and $\varepsilon_1(\Omega)$ are the dielectric constants in the wells and barriers, respectively.

Its solutions $\Omega_{\lambda\vec{q}} = \hbar\omega_{\lambda\vec{q}}$ define the energy spectrum of interface phonons. For the nondegenerated case, the number of phonon modes (λ) is equal to the twice number of all interfaces between nano-structure layers.

Quantizing the polarization field using the known quantum mechanics method [9], we obtain the Hamiltonian of interface phonons

$$\widehat{H}_I = \sum_{\lambda, \vec{q}} \Omega_{\lambda\vec{q}} \left(b_{\lambda\vec{q}}^+ b_{\lambda\vec{q}} + \frac{1}{2} \right), \quad \lambda = 1, \dots, 8 \quad (22)$$

and the Hamiltonian of electron-I-phonon interaction

$$\widehat{H}_{e-I} = -e\Phi(\vec{\rho}, z) = - \sum_{\lambda, \vec{q}, j} eC_\lambda(q) \varphi_j(\lambda, q, z) e^{i\vec{q}\vec{\rho}} \left(b_{\lambda\vec{q}} + b_{\lambda, -\vec{q}}^+ \right) \quad (23)$$

in coordinate representation over the electron variables $(\vec{\rho}, z)$ and in the representation of occupation numbers over the phonon variables with operators $b_{\lambda\vec{q}}^+$, $b_{\lambda\vec{q}}$, satisfying commutative relationships and with the known coefficients $C_\lambda(q)$ and functions $\varphi_j(\lambda, q, z)$.

Performing the transition to the representation of electron occupation numbers in (23) using the quantized wave function (12), we obtain the Hamiltonian of electron-I-phonon interaction in the representation of the second quantization over all variables of the system

$$\widehat{H}_{e-I} = \sum_{\substack{\bar{n}_1, \bar{n}, \vec{k} \\ \lambda, \vec{q}}} F_{\bar{n}_1 \bar{n}}(\lambda, \vec{q}) a_{\bar{n}_1 \vec{k} + \vec{q}}^+ a_{\bar{n} \vec{k}} (b_{\lambda \vec{q}} + b_{\lambda, -\vec{q}}^+), \quad (24)$$

where binding functions

$$F_{\bar{n}_1 \bar{n}}(\lambda, \vec{q}) = - \sqrt{\frac{8\pi\Omega a_b \text{Ry}}{L^2 q N(\lambda, q)}} \sum_{j=1}^5 \int_{z_{j-1}}^{z_j} \Psi_{\bar{n}_1 j}^*(z) \Psi_{\bar{n} j}(z) [\alpha_j(\Omega_{\lambda q}) e^{-qz} + \beta_j(\Omega_{\lambda q}) e^{qz}] dz \quad (25)$$

contain the normality coefficient

$$N(\lambda, q) = \sum_{j=1}^5 \omega_{\lambda=1}^{(q=0)} \frac{\partial \mathcal{E}_j(\omega)}{\partial \omega} \Big|_{\omega=\omega_{\lambda}(q)} \left[\beta_j^2(\Omega_{\lambda \vec{q}}) (e^{2qz_j} - e^{2qz_{j-1}}) - \alpha_j^2(\Omega_{\lambda \vec{q}}) (e^{-2qz_j} - e^{-2qz_{j-1}}) \right]. \quad (26)$$

Here, $\text{Ry} = e^2/2a_b$, $\Omega = \hbar\omega_{\lambda=1}^{(q=0)}$, a_b is Bohr radius. Integral in (25) is analytically calculated but we do not present it due to its sophisticated form.

We should note that at $q \rightarrow 0$, the binding function $F_{\bar{n}_1 \bar{n}}(\lambda, \vec{q}) \sim q^{-1/2}$ and, thus, a further integration in MO is not divergent.

The obtained Hamiltonian of electron-I-phonon system in three-barrier RTS

$$H = H_e + H_I + H_{e-I} \quad (27)$$

allows us to calculate the Fourier-image of electron Green's function in the quasi-stationary part of the spectrum according to the rules of Feynman-Pines diagram technique [9], at the finite temperature, when Dyson equation is valid

$$G_n(\vec{k}, \hbar\omega) = \left[\hbar\omega - E_{n\vec{k}} - M_n(\hbar\omega, \vec{k}) \right]^{-1} \quad (28)$$

with mass operator (MO) $M_n(\hbar\omega, \vec{k})$ calculated (due to the weak electron-I-phonon binding) in one-phonon approximation ($\eta \rightarrow \pm 0$)

$$M_n(\hbar\omega, \vec{k}) = \sum_{\bar{n}_1, \lambda, \vec{q}} F_{n\bar{n}_1}^*(\lambda, \vec{q}) F_{\bar{n}_1 n}(\lambda, \vec{q}) \left[\frac{1 + \nu_{\lambda \vec{q}}}{\hbar\omega - E_{\bar{n}_1}(\vec{k} + \vec{q}) - \Omega_{\lambda \vec{q}} + i\eta} + \frac{\nu_{\lambda \vec{q}}}{\hbar\omega - E_{\bar{n}_1}(\vec{k} + \vec{q}) + \Omega_{\lambda \vec{q}} + i\eta} \right], \quad (29)$$

where $\nu_{\lambda \vec{q}} = \left[e^{\Omega_{\lambda \vec{q}}/\hbar kT} - 1 \right]^{-1}$ is the average number of I-phonons occupation numbers.

Further, using this MO, we study the contributions of different mechanisms of electron-I-phonon interaction into renormalized spectral parameters (energy shifts (Δ_n) and decay rates (Γ_n)) of n -th electron state. In experiments [1–3], the electrons move perpendicularly to the planes of three-barrier RTS, thus in MO (25) we put $\vec{k} = 0$ and neglect the frequency dependence of MO in the vicinity of E_n energies taking into account a weak electron phonon binding (further proven by numeric calculations). To distinguish the role of different mechanisms of electron-I-phonon interaction, one should extract the real and imaginary part in MO

$$M_n(\vec{k} = 0, \hbar\omega = E_n) = \text{Re}M_n(\vec{k} = 0, \hbar\omega = E_n) + i\text{Im}M_n(\vec{k} = 0, \hbar\omega = E_n) = \Delta_n - i\Gamma_n/2, \quad (30)$$

as well as the terms describing the partial contributions of I-phonons due to interaction with electrons from different states

$$\Delta_n = \Delta_{nn} + \Delta_{nd} + \Delta_{nc}, \quad \Gamma_n = \Gamma_{nn} + \Gamma_{nd} + \Gamma_{nc}, \quad (31)$$

where Δ_{nn} is the partial shift of the n -th state due to the intra-level interaction within I-phonons

$$\Delta_{nn} = \left(\frac{L}{2\pi} \right)^2 \sum_{\lambda, \pm} \mathcal{P} \int \int d^2 \vec{q} (E_n - E_{n\vec{q}} \mp \Omega_{\lambda \vec{q}})^{-1} \left| F_{nn}^{(\lambda, \vec{q})} \right|^2 \left(\nu_{\lambda \vec{q}} + \frac{1}{2} \pm \frac{1}{2} \right), \quad (32)$$

Γ_{nn} is the decay rate of the n -th state due to the intra-level interaction within I-phonons

$$\Gamma_{nn} = \frac{L^2}{2\pi} \sum_{\lambda, \pm} \int \int d^2 \vec{q} [\delta(E_n - E_{n\vec{q}} \mp \Omega_{\lambda\vec{q}})] |F_{nn}^{(\lambda, \vec{q})}|^2 \left(v_{\lambda\vec{q}} + \frac{1}{2} \pm \frac{1}{2} \right), \quad (33)$$

$\Delta_{n(\frac{c}{d})}$ and $\Gamma_{n(\frac{c}{d})}$ are the partial shifts and decay rates of the n -th state due to the interaction within I-phonons with all (except the n -th) states of quasi-discrete (d) spectrum ($\Delta_{nd} = \sum_{n_1 \neq n} \Delta_{nn_1}$, $\Gamma_{nd} = \sum_{n_1 \neq n} \Gamma_{nn_1}$) and with the states of continuum (c) ($\Delta_{nc} = \sum_{k_z} \Delta_{nk_z}$, $\Gamma_{nc} = \sum_{k_z} \Gamma_{nk_z}$),

$$\begin{aligned} \Delta_{n(\frac{c}{d})} - i\Gamma_{n(\frac{c}{d})} &= \left(\frac{L}{2\pi} \right)^2 \sum_{\substack{k_z \\ n_1 \neq n}} \sum_{\lambda, \pm} \int \int d^2 \vec{q} F_{n(k_z)}^*(\lambda, \vec{q}) F_{n(k_z)}(\lambda, \vec{q}) \left(v_{\lambda\vec{q}} + \frac{1}{2} \pm \frac{1}{2} \right) \\ &\times \left[\mathcal{P} \left(E_n - E_{n(k_z)} \mp \Omega_{\lambda\vec{q}} \right)^{-1} - 2\pi i \delta \left(E_n - E_{n(k_z)} \mp \Omega_{\lambda\vec{q}} \right) \right]. \end{aligned} \quad (34)$$

Symbol \mathcal{P} in formulas (32), (34) means that the respective integrals are taken as Cauchy principal values.

Using the developed theory, we numerically calculated the energies renormalized due to phonons ($\tilde{E}_n = E_n + \Delta_n$) and decay rates (Γ_n) of electron states in quasi-discrete spectrum at the fixed physical and geometrical parameters of three-barrier RTS.

3. Parameters of electron spectrum as functions of temperature and design of three-barrier RTS (GaAs/Al_xGa_{1-x}As)

The complete and partial shifts and decay rates of electron spectrum in three-barrier RTS were calculated for GaAs/Al_xGa_{1-x}As nano-structure, being the active element of the experimentally investigated QCD [2, 3, 17]. The physical parameters are presented in table 1.

Table 1. Physical parameters of nanostructures.

	ϵ_∞	$\hbar\omega_L$, meV	$\hbar\omega_T$, meV	m_e/m	U , meV
GaAs	10.89	36.25	33.29	0.067	
Al _{0.15} Ga _{0.85} As	10.48	35.31	33.19	0.079	120
Al _{0.45} Ga _{0.55} As	9.66	33.66	32.77	0.104	320

In figure 2, the electron spectrum as the function of the position of the inner barrier with respect to the outer ones is presented at different Al concentrations: $x = 0.15$ and low potential barrier $U = 120$ meV (a); $x = 0.45$ and high potential barrier $U = 320$ meV (b). The thicknesses of the inner barriers ($b = 1.13$ nm) and the sum of both well widths ($a = a_1 + a_2 = 13.9$ nm) are the same for the both structures. The figure proves that independently of Al concentration, the quasi-discrete energy levels (E_n) qualitatively similarly depend on the position of the inner barrier (fixed by the width of input well (a_1)): the energies E_n are the symmetric functions with respect to the average position of the inner barrier in the common well ($a_1 = a_2 = a/2$) with n maxima. Two nearest operating levels (E_1, E_2) have one maximum at $a_1 = a/2$ and two maxima — at $a_1 = a/4, 3a/4$, respectively. The anti-crossing is observed at $a_1 = a/2$, where the distance between E_2 and E_1 is minimal, due to the presence of two wells in a three-barrier RTS.

In figure 3, the energy spectra of interface phonons ($\Omega_{\lambda\vec{q}}$) are presented for the both three-barrier RTS (a), (b). The spectra contain two groups having four modes of energies of a weak dispersion. The high-energy group is placed between the energies of longitudinal phonons ($\Omega_{L_1}, \Omega_{L_2}$) and the low-energy group — between the energies of transversal phonons ($\Omega_{T_1}, \Omega_{T_2}$) of the respective layers. In each group, the pair of modes with a higher energy has a negative dispersion while with lower energy — positive dispersion. The position of the inner barrier with respect to the outer ones weakly effects the magnitude

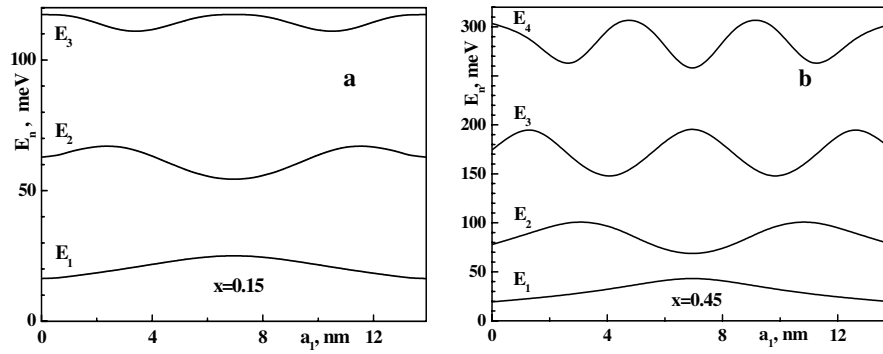


Figure 2. Energy spectrum of electron (E_n) noninteracting with phonons as a function of the inner barrier position (a_1) at $x = 0.15$ and $U = 120$ meV (a) and $x = 0.45$ and $U = 320$ meV (b); $a = 13.9$ nm, $b = 1.13$ nm.

of the dispersion: $\Omega_{\lambda\bar{q}}$ varies at 2–3 % at big q and the energies become almost the same at a small q . An increase of Al concentration in the barriers does not qualitatively vary the dispersion of all phonon modes but increases its magnitude at a small quasi-momentum.

In order to study the effect of electron-I-phonon interaction on the magnitude of the electromagnetic field energy absorbed by a nano-structure ($\tilde{E}_{21} = \tilde{E}_2 - \tilde{E}_1$) arising due to the quantum transition from the first ($|1\rangle$) into the second ($|2\rangle$) quasi-stationary state, we calculated the complete and partial shifts (Δ_n , Δ_{nd} , Δ_{nc}) and decay rates (Γ_n , Γ_{nd} , Γ_{nc}) of two operating states ($n = 1, 2$). The results are presented in figure 4 at $T = 0$ and 300 K for a nano-structure (a) because Al concentration causes their small quantitative changes for a nano-structure (b).

Figure 4 (a), (b) proves that at cryogenic temperatures (formally at $T = 0$ K), the both operating states ($|1\rangle$ and $|2\rangle$) shift into the region of smaller energies ($\Delta_1, \Delta_2 < 0$) independently of three-barrier RTS design due to electron-I-phonon interaction. The magnitudes of complete shifts nonlinearly depend on the position of the inner barrier (a_1) and are of the same order. The complete shifts are mainly produced by intra-level interactions with partial shifts Δ_{11} , Δ_{22} . The shifts Δ_{1d} , Δ_{2d} are produced by inter-level interaction due to all states of a quasi-discrete spectrum and are smaller than Δ_{11} , Δ_{22} . Only at some magnitudes of a_1 , the partial shifts Δ_{22} and Δ_{2d} have correlating magnitudes. The partial shifts (Δ_{1c} , Δ_{2c}) are caused by the interaction with the continuum states and are smaller or much smaller than the others. The shifts are negative because at $T = 0$ K only virtual phonons exist in the system.

The decay rate of electron spectrum (Γ_n) is regulated by the energy conservation law which, as it is clear from MO (23) at $T = 0$ K, is determined by δ -function $\delta(E_n - E_{n_1} - \Omega_{\lambda\bar{q}} - \hbar^2 q^2 / 2m)$. Consequently,

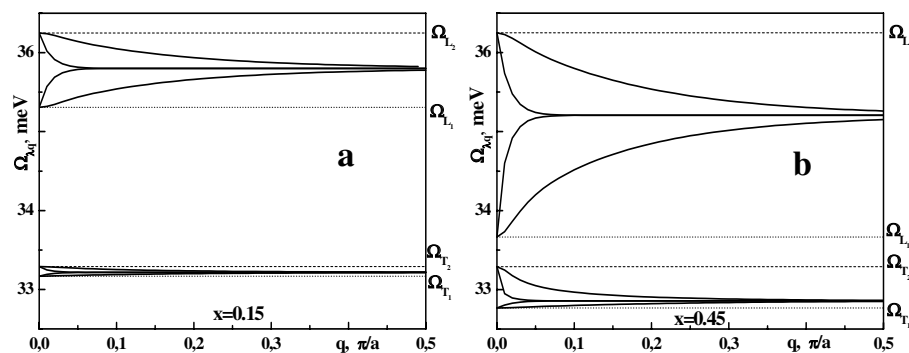


Figure 3. Energy spectra ($\Omega_{\lambda\bar{q}}$) of interface phonons uncoupling with electrons as a function of quasi-momentum (q) at $x = 0.15$ and $U = 120$ meV (a) and $x = 0.45$ and $U = 320$ meV (b); $a = 13.9$ nm, $b = 1.13$ nm; Ω_{L_1} , Ω_{L_2} are the energies of longitudinal phonons, Ω_{T_1} , Ω_{T_2} are the energies of transversal phonons in the wells (1) and barriers (2).

and $\Gamma_{nm_1} \neq 0$. In the last case, only the inter-level interaction due to phonons causes the finite decay of higher states at cryogenic temperatures ($T = 0$ K).

Figure 4 c presents the mentioned reasons determining the decay rates of electron states at $T = 0$ K. In the figure one can see the decay rate ($\Gamma_2 = \Gamma_{21}$) of the energy of quantum transition $E_{21} = E_2 - E_1$ detected at the absorption of electromagnetic wave, as a function of design of three-barrier RTS (a_1) and the stripe, where all modes of I-phonon energies ($\Omega_{\lambda\bar{q}}$) are located. The figure proves that the decay rate of the first state ($|1\rangle$) is absent ($\Gamma_1 = 0$) and, as far as $\Gamma_{22} = 0$, the decay rate of the second state ($|2\rangle$) is caused only by the inter-level interaction due to phonons ($\Gamma_2 = \Gamma_{21}$). Thus, $\Gamma_2 = 0$ in the range $4.75 \leq a_1 \leq 9.15$ where $E_{21} \leq \Omega_{\lambda\bar{q}}$ and $\Gamma_2 \neq 0$ in the ranges $0 \leq a_1 \leq 4.75$ and $9.15 \leq a_1 \leq 13.9$ where $E_{21} > \Omega_{\lambda\bar{q}}$.

At the finite temperature, the average occupation number of phonon states is not equal to zero ($\nu_{\lambda\bar{q}} \neq 0$). Therefore, as it is clear from MO (23), the spectral parameters of both operating states are produced not only by virtual (as at $T = 0$ K) but also by real I-phonons, both in the processes of their creation, described by the first term of MO proportional to $(1 + \nu_{\lambda\bar{q}})$ and in the processes of their annihilation, described by the second term of MO proportional to $\nu_{\lambda\bar{q}}$.

In figure 4 (d), (e), (f), the complete and partial shifts ($\Delta_n^T, \Delta_{nd}^T, \Delta_{nc}^T$) and decay rates ($\Gamma_n^T, \Gamma_{nd}^T, \Gamma_{nc}^T$) of the operating electron states ($n = 1, 2$) are presented at $T = 300$ K. It is clear that the temperature weakly changes the shapes and magnitudes of both states shifts depending on the position of the inner barrier (a_1). The decay rates (Γ_1^T, Γ_2^T) are produced by partial contributions of intra-level ($\Gamma_{11}^T, \Gamma_{22}^T$) and inter-level ($\Gamma_{12}^T, \Gamma_{21}^T$) interactions with I-phonons in the processes of their creation and annihilation.

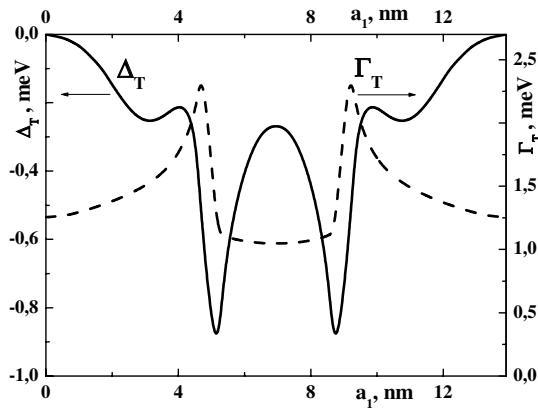


Figure 5. A complete shift (Δ_T) and the decay rate (Γ_T) as a function of the inner barrier position (a_1) at $T = 300$ K; $a = 13.9$ nm, $b = 1.13$ nm.

In figure 5, a complete shift ($\Delta_T = \Delta_2^T - \Delta_1^T$) and decay rate ($\Gamma_T = \Gamma_1^T + \Gamma_2^T$) of energy ($\tilde{E}_{21} = E_{21} + \Delta_T$) in the process of electromagnetic wave absorption as functions of the inner barrier position (a_1) is presented at $T = 300$ K. The both functions are strongly nonlinear while the respective magnitudes are not big.

We should note that sharp minima at the curves of all shifts and respective maxima at the curves of the decay rates (figures 4, 5) are mainly caused by a bigger contribution of inter-level interaction between the second and third level in those two configurations of a three-barrier RTS where the anticrossing arises between them.

According to physical considerations, the decay increases and the magnitude of the detected energy weakly decreases when the temperature increases, which qualitatively correlates with the experimental results [17].

It is clear that one should consider in the model the confined polarization and acoustic phonons in order to quantitatively compare the theoretical and experimental data. This rather complicated and sophisticated work will be done in further investigations based on the approach proposed in this paper.

4. Main results and conclusions

From the first principles (without any fitting parameters), we obtained the Hamiltonian of electron-I-phonon system in the representation of the second quantization over all variables for a three-barrier RTS. The renormalized electron spectrum was calculated at cryogenic and room temperatures using the thermo-dynamical Green's functions method. For GaAs/Al_xGa_{1-x}As nano-structure, we studied in detail the effect of various mechanisms of electron-phonon interaction (intra-level and inter-level with quasi-discrete and continuum spectrum) at the formation of energy shifts and decay rates of electron states depending on the geometric design of three-barrier RTS.

The energies of electron states, the energy of electromagnetic field absorbed by a three-barrier RTS which is an active element of QCD, at quantum transition between the first and the second states, the

shifts of the energies and decay rates due to the electron-I-phonon interaction are not big over the magnitude, while nonlinear functions depend on the position of the inner barrier between the outer barriers.

It is proven that independently of the geometric design of a three-barrier RTS, an increase of temperature causes bigger decay rates of both operating electron states and their shift into the low-energy region. The shift of the first level is smaller than that of the second one. Thus, being detected by QCD, the energy of electromagnetic field absorbed at a quantum transition decreases, which qualitatively correlates with the experiment.

References

1. Luo H., Liu H.C., Song C.Y., Wasilewski Z.R., Appl. Phys. Lett., 2005, **86**, 231103; doi:10.1063/1.1947377.
2. Hofstetter D., Graf M., Aellen T., Faist J., Appl. Phys. Lett., 2006, **89**, 061119; doi:10.1063/1.2269408.
3. Giorgetta F.R., Baumann E., Graf M., Yang Q., Manz Ch., Kohler K., Beere H.E., Ritchie D.A., Linfield E., Davies A.G., Fedoryshyn Y., Jackel H., Fischer M., Faist J., Hofstetter D., IEEE J. Quantum Electron., 2009, **45**, No. 8, 1039; doi:10.1109/JQE.2009.2017929.
4. Yu C.H., Zhang B., Shen S.C., Lu W., Liu H.C., Fang Y.-Y., Dai J.N., Chen C.Q., Appl. Phys. Lett., 2010, **97**, 022102; doi:10.1063/1.3462300.
5. Tkach M.V., Seti Ju.O., Ukr. J. Phys., 2013, **58**, No. 2, 182.
6. Tkach N.V., Seti Ju.A., Semiconductors, 2011, **45**, No. 3, 376; doi:10.1134/S1063782611030195.
7. Tkach M.V., Seti Ju.O., Voitsekhivska O.M., Zegrya G.G., Rom. J. Phys., 2012, **57**, 620.
8. Mori N., Ando T., Phys. Rev B, 1989, **40**, 6175; doi:10.1103/PhysRevB.40.6175.
9. Tkach M.V., Quasiparticles in nanoheterosystems. Quantum dots and wires, Chernivtsi University Press, Chernivtsi, 2003.
10. Shi J.J., Sanders B.C., Pan S.H., Eur. Phys. J. B, 1998, **4**, 113; doi:10.1007/s100510050357.
11. Yan Z.W., Liang X.X., Int. J. Mod. Phys. B, 2001, **15**, No. 27, 3539; doi:10.1142/S0217979201007804.
12. Yan Z.W., Ban S.L., Liang X.X., Int. J. Mod. Phys. B, 2003, **17**, No. 31, 6085; doi:10.1142/S0217979203023653.
13. Wu B.H., Cao J.C., Xio G.Q., Lio H.C., Eur. Phys. J. B, 2003, **33**, 9; doi:10.1140/epjb/e2003-00135-2.
14. Huang W.D., Wei S.Y., Ren Y.J., Wang Y.H., Int. J. Mod. Phys. B, 2007, **21**, No. 25, 4407; doi:10.1142/S0217979207037843.
15. Jiraushek C., Kubis T., Appl. Phys. Rev., 2014, **1**, 011307; doi:10.1063/1.4863665.
16. Gao X., Botez D., Knezevic I., J. Appl. Phys., 2007, **101**, 063101; doi:10.1063/1.2711153.
17. Gendron L., Carras M., Huynh A., Ortiz V., Appl. Phys. Lett., 2004, **85**, No. 14, 2824; doi:10.1063/1.1781731.

Вплив інтерфейсних фононів на електронні робочі стани трибар'єрної резонансно-тунельної наноструктури як активної зони квантового каскадного детектора

М.В.Ткач, Ю.О.Сеті, Ю.Б. Гринишин, О.М.Войцехівська

Чернівецький національний університет ім. Ю. Федьковича,
вул. Коцюбинського, 2, 58012 Чернівці, Україна

З перших принципів у моделі ефективних мас та поляризаційного континууму встановлено гамільтоніан системи електронів взаємодіючих з інтерфейсними фононами у трибар'єрній резонансно-тунельній структурі. Методом функцій Гріна розраховано температурні зміщення й загасання найнижчих (робочих) електронних станів у залежності від геометричної конфігурації наносистеми GaAs/Al_xGa_{1-x}As як активної зони квантового каскадного детектора. Встановлено, що незалежно від температури системи енергія квантового переходу в процесах поглинання електромагнітного поля є нелінійною слабозмінною функцією від положення внутрішнього відносно зовнішніх бар'єра наносистеми.

Ключові слова: резонансно-тунельна наноструктура, інтерфейсні фонони, квантовий каскадний детектор